Coral-algae metabolism and diurnal changes in the CO_2-carbonate system of bulk sea water

Paul L. Jokiel, Christopher P. Jury and Ku'ulei S. Rodgers

Hawaii Institute of Marine Biology, University of Hawaii, Kaneohe, HI, United States

Corresponding author
Paul L. Jokiel, jokiel@hawaii.edu

ABSTRACT

Precise measurements were conducted in continuous flow seawater mesocosms located in full sunlight that compared metabolic response of coral, coral-macroalgae and macroalgae systems over a diurnal cycle. Irradiance controlled net photosynthesis (P_{net}), which in turn drove net calcification (G_{net}), and altered pH. P_{net} exerted the dominant control on [CO_3^{2-}] and aragonite saturation state (Ω_{arag}) over the diel cycle. Dark calcification rate decreased after sunset, reaching zero near midnight followed by an increasing rate that peaked at 03:00 h. Changes in Ω_{arag} and pH lagged behind G_{net} throughout the daily cycle by two or more hours. The flux rate P_{net} was the primary driver of calcification. Daytime coral metabolism rapidly removes dissolved inorganic carbon (DIC) from the bulk seawater and photosynthesis provides the energy that drives G_{net} while increasing the bulk water pH. These relationships result in a correlation between G_{net} and Ω_{arag}, with Ω_{arag} as the dependent variable. High rates of H^+ efflux continued for several hours following mid-day peak G_{net} suggesting that corals have difficulty in shedding waste protons as described by the Proton Flux Hypothesis. DIC flux (uptake) followed P_{net} and G_{net} and dropped off rapidly following peak P_{net} and peak G_{net} indicating that corals can cope more effectively with the problem of limited DIC supply compared to the problem of eliminating H^+. Over a 24 h period the plot of total alkalinity (A_T) versus DIC as well as the plot of G_{net} versus Ω_{arag} revealed a circular hysteresis pattern over the diel cycle in the coral and coral-algae mesocosms, but not the macroalgae mesocosm. Presence of macroalgae did not change G_{net} of the corals, but altered the relationship between Ω_{arag} and G_{net}. Predictive models of how future global changes will effect coral growth that are based on oceanic Ω_{arag} must include the influence of future localized P_{net} on G_{net} and changes in rate of reef carbonate dissolution. The correlation between Ω_{arag} and G_{net} over the diel cycle is simply the response of the CO_2-carbonate system to increased pH as photosynthesis shifts the equilibria and increases the [CO_3^{2-}] relative to the other DIC components of [HCO_3^-] and [CO_2]. Therefore Ω_{arag} closely tracked pH as an effect of changes in P_{net}, which also drove changes in G_{net}. Measurements of DIC flux and H^+ flux are far more useful than concentrations in describing coral metabolism dynamics. Coral reefs are systems that exist in constant disequilibrium with the water column.

INTRODUCTION

Recent field experiments have identified the need for accurate metabolic measurements on coral reefs at short time intervals in order to detect subtle aspects such as phase lags between the concentrations and flux rates of major metabolic parameters over the diurnal cycle (e.g., *Shamberger et al., 2011*; *McMahon et al., 2013*). There is a need to test the assumption that night calcification is very low and constant and that calcification is limited by inorganic carbon concentration in the form of CO_3^{2-}. Finely detailed diurnal metabolic measurements are difficult to obtain in field investigations. For example, *Falter et al. (2012)* based their extensive study at Nigaloo Reef, NW Australia on a total of 13 summer measurements of calcification taken at various times over 12 days between 08:00 and 18:00 with one night measurement at 21:00. The following winter a total of 11 more measurements were made over 4 days with no night measurements. These data are valuable, but do not provide the diurnal resolution that is needed to fully describe coral and coral reef metabolism. Thus we undertook a laboratory investigation that would provide such data.

BACKGROUND INFORMATION

The term Ω_{arag} is defined as:

$$\Omega_{\text{arag}} = \frac{[Ca^{2+}][CO_3^{2-}]}{K_{sp}} \tag{1}$$

where K_{sp} is the solubility constant of aragonite. The $[Ca^{2+}]$ in normal present-day oceanic seawater is essentially constant at 10.3 mmol kg^{-1} SW, normalized to salinity. Likewise, K_{sp} is a constant (at a given temperature, pressure, and salinity), so in shallow oceanic waters Ω_{arag} is directly proportional to $[CO_3^{2-}]$. Changes in seawater pH shift the equilibria between the various forms of dissolved inorganic carbon (DIC) as follows:

$$CO_2 + H_2O \Leftrightarrow H^+ + HCO_3^- \Leftrightarrow 2H^+ + CO_3^{2-}. \tag{2}$$
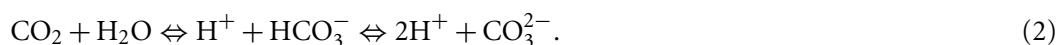
Calcification inevitably produces an excess of H^+ and thus reduces total alkalinity (A_T) by two moles for every mole of CaCO$_3$ precipitated (*Kinsey, 1978*; *Smith & Kinsey, 1978*). The correct equations for calcification are as follows:

$$Ca^{2+} + (CO_2 + H_2O) \Leftrightarrow CaCO_3 + 2H^+ \tag{3}$$

$$\updownarrow$$

$$Ca^{2+} + (H^+ + HCO_3^-) \Leftrightarrow CaCO_3 + 2H^+ \tag{4}$$

$$\updownarrow$$

$$Ca^{2+} + (2H^+ + CO_3^{2-}) \Leftrightarrow CaCO_3 + 2H^+ \tag{5}$$

Equations 3–5 are written in two dimensions with a red arrow showing the relationship between the carbonate species (in parentheses) that shift with the changes in $[H^+]$

described as Eq. (2). Dissolution is the reverse of the calcification reaction. Net calcification (G_{net}) is the sum of calcification (positive flux) and dissolution (negative flux). When the equations are written correctly in this manner the importance of protons becomes apparent with two moles of H^+ produced for every mole of $CaCO_3$ precipitated regardless of which form of dissolved inorganic carbon (DIC) is involved.

The following equations describe photosynthetic carbohydrate formation from the various available CO_2 species:

$$(CO_2 + H_2O) \Leftrightarrow CH_2O + O_2 \tag{6}$$

$$\updownarrow$$

$$(H^+ + HCO_3^-) \Leftrightarrow CH_2O + O_2 \tag{7}$$

$$\updownarrow$$

$$(2H^+ + CO_3^{2-}) \Leftrightarrow CH_2O + O_2. \tag{8}$$

The photosynthesis equations are also written in two dimensions with the red arrows showing changes in distribution of species that occurs (Eq. (2)) with shifts in pH. Note that photosynthesis increases pH (lowers $[H^+]$) while the reverse reaction of respiration decreases pH (increases $[H^+]$). Net photosynthesis (P_{net}) is the sum of photosynthesis (positive flux) and respiration (negative flux). Unlike calcification-dissolution, photosynthesis-respiration does not alter total alkalinity (A_T).

In sum, photosynthesis and calcification both lower the seawater DIC, while respiration and $CaCO_3$ dissolution raise DIC. Only the precipitation or dissolution of $CaCO_3$ significantly alters A_T. Consequently, changes in $[A_T]$ can be used to calculate calcification and dissolution rates (G_{net}), and is widely used in this regard. Photosynthesis and respiration can radically alter $[H^+]$ and thus can alter relative concentration of CO_3^{2-}, HCO_3^- and CO_2. Coral calcification is a biological process that is heavily influenced by the associated processes of photosynthesis and respiration (P_{net}) that modify pH. Protons can be considered a waste product of calcification Eqs. (3)–(5) and O_2 a waste product of photosynthesis Eqs. (6)–(8).

METHODS AND MATERIALS

A mesocosm experiment was undertaken in order to precisely measure the changes in bulk sea water chemistry and material flux caused by coral and algae metabolism over a diurnal cycle. The experiment was conducted in the flow-through mesocosm system at the Hawaii Institute of Marine Biology, Kaneohe Bay, Oahu, Hawaii. The mesocosm system has been described previously in detail (*Jokiel et al., 2008*; *Andersson et al., 2009*; *Jokiel, Bahr & Rodgers, in press*). The fiberglass mesocosm tanks were located in full sunlight and supplied with flowing seawater pumped from approximately 2 m depth at the edge of the Coconut Island coral reef. Each mesocosm received a flow of approximately 7.5 to 8.5 l min^{-1} resulting in a turnover rate of approximately 1 h. Solar input at the site

Table 1 Mesocosm volume and biomass of the coral *Montipora capitata* and the macroalga *Gracillaria salicornia*.

Mesocosm	Biomass	Tank dimensions in cm			
		Length	Width	Water depth	Volume (l)
Coral only	7,555 g buoyant weight coral	117	117	38	520
Coral plus Algae	7,555 g buoyant weight coral, and 3,151 g of *Gracillaria salicornia*	117	117	38	520
Algae	3,151 g of *Gracillaria salicornia*	117	117	35	479

was monitored with a LiCor Brand Quantameter (Li-Cor Inc., Lincoln, NE, USA), which measured photosynthetically active radiance (PAR) between 400 nm and 700 nm.

Three continuous flow mesocosms were used for this experiment. The first mesocosm ("Coral only") was loaded with 7.6 kg buoyant weight of the reef coral *Montipora capitata* for close to 100% coverage of the bottom (Table 1). This buoyant weight translates into 11.5 kg dry skeletal weight (*Jokiel, Maragos & Franzisket, 1978*). The second mesocosm ("Coral plus Algae") contained the same weight of live coral plus 3.1 kg wet weight of the macroalgae *Gracillaria salicornia*. The third mesocosm ("Algae only") was loaded with the same weight of the macroalgae. A small biomass of calcifying organisms was present on the macroalgae in the form of epiphytes that were not removed. Dead skeletal material and sediment were excluded from all three mesocosms to reduce the complicating effect of decalcification of carbonates and related processes on G_{net} (*Murillo, Jokiel & Atkinson, 2014*). The organisms in the mesocosms were allowed to acclimate to mesocosm conditions for one week prior to the experiment.

This experimental design allows the three treatments to be run simultaneously which eliminates the between-treatment variance due to solar irradiance, temperature and other factors that would occur if they were run at different times. The functioning of each community under identical conditions serves as a control and as a contrast to the other two communities. Response of these communities to the diurnal irradiance cycle and variation in other factors is non-linear, so the data were analyzed by graphical comparison and integrated response of 24 h P_{net} and G_{net}.

The seawater inflow enters at the bottom in the center of each mesocosm (see *Smith et al., 1977* for details on the mesocosm system) at a vertical angle, which ensures a uniform and well-mixed system. Maintaining seawater inflow of reef water at constant rates insured that natural fluctuations in seawater chemistry observed on the adjacent reef during the diel cycle was preserved during the experiment. Water chemistry was sampled hourly from 06:00 on 24 April to 07:00 on 25 April 2012 at the inlet and outlet and the flow rate recorded. During the experiment the flow rate was precisely measured every hour for each mesocosm and inlet-outlet chemistry was determined. Temperature and salinity were measured with a YSI Brand Model 30 salinity–conductivity–temperature meter (± 0.1 °C; ± 0.1 ppt). Dissolved oxygen (DO) was measured with a YSI Brand Model 57 Dissolved Oxygen Meter (± 0.2 mg l^{-1}), and pH$_{NBS}$ with an Accumet AP72
pH/mV/temperature meter verified spectrophotometrically using *m*-cresol purple dye according to SOP 7 (*Dickson, Sabine & Christian, 2007*). A_T was measured using a Titrino Model 877 titrator system. Alkalinity samples were equilibrated to 25 °C and run within an hour of being taken. Accuracy and precision of the titrations was confirmed with certified reference materials (CRM Batch 129) from the Dickson Laboratory, Scripps Institution of Oceanography which verified that our measurements of A_T were accurate to within 0.18% of the Dickson CRM value. All carbonate parameters were calculated using the program CO2SYS (*Pierrot, Lewis & Wallace, 2006*) and stoichiometric dissociation constants defined by *Mehrbach et al. (1973)* and refit by *Dickson & Millero (1987)*.

The mesocosms are well mixed systems and can be represented by a simple box model *Andersson et al. (2009)*. Changes in total alkalinity (A_T) are attributed to calcification or carbonate dissolution *Murillo, Jokiel & Atkinson (2014)*. The net calcification (G_{net}) can be easily calculated from Eq. (9) by measuring the amount of material in the inflowing (F_{in}) and outflowing (F_{out}) seawater, and the change per unit time in the mesocosm seawater between consecutive sampling times. For G_{net} the resulting value is divided by 2 because two moles of A_T are produced for every mole of $CaCO_3$ precipitated (calcification) or removed (dissolution) as shown by Eqs. (3)–(5).

$$G_{net} = \frac{F_{in}A_T - F_{out}A_T - \frac{dA_T}{dt}}{2}. \tag{9}$$

P_{net} was measured in a similar manner using O_2 concentration, with one mole of carbon being produced for every mole of O_2 produced as shown by Eqs. (6)–(8). Likewise DIC and H^+ were calculated using Eqs. (11) and (12).

$$P_{net} = F_{in}O_2 - F_{out}O_2 - \frac{dO_2}{dt} \tag{10}$$

$$DIC_{net} = F_{in}DIC - F_{out}DIC - \frac{dDIC}{dt} \tag{11}$$

$$H_{net}^+ = F_{in}H^+ - F_{out}H^+ - \frac{dH^+}{dt}. \tag{12}$$

RESULTS AND DISCUSSION

All of the measurements taken during this experiment are shown in Table 2.

Calcification over the 24 h period (Fig. 1) shows the diurnal pattern related to irradiance, light enhanced calcification and dark calcification. Values for G_{net} are high due to the large biomass of live coral, high solar irradiance in the shallow mesocosms and absence of sediment or dead carbonate skeleton which are subject to dissolution. G_{net} in the "Corals only" and "Corals plus Algae" treatments track each other closely. Light saturation of calcification did not occur up to the maximum irradiance which exceeded 1,500 µmole photons m^{-2} s^{-1}. This value is many times higher than that supplied by the artificial light typically used is most laboratory studies of coral calcification. Calcification rate is very low in the "Algae only" treatment due to low biomass of calcifying organisms, which are made up of various calcifying epiphytes. Low-levels of dark calcification occur at

Table 2 Measurements made during the mesocosm experiment of April 24–25, 2012.

Time	Irradiance μmole photons m^{-2} h^{-1}	Salinity o/oo	Inlet—all mesocosms				Outlet Algae only mesocosm							
			pH	A_T	Temp °C	O$_2$ In mg l^{-1}	Flow liters min^{-1}	pH	A_T	Temp °C	O$_2$ Out mg l^{-1}	G_{net}	P_{net}	Mean Ω_{arag}
6:00	0	34.8	7.95	2196.5	23.1	6.0	7.50	7.93	2196.0	23.0	6.0			
7:00	56	34.9	7.95	2198.3	23.5	6.0	7.50	7.93	2196.7	23.2	6.1	0.3	22	2.49
8:00	222	34.8	8.03	2199.0	23.5	6.0	7.50	8.01	2193.5	23.3	6.4	1.0	127	2.70
9:00	464	34.9	8.03	2185.0	23.5	6.3	7.50	8.02	2190.7	23.4	7.1	0.0	340	2.93
10:00	854	34.8	8.06	2200.3	23.3	6.9	7.33	8.06	2182.9	23.6	8.0	1.6	539	3.09
11:00	1619	34.8	8.06	2206.2	23.9	6.6	7.50	8.11	2198.5	23.6	8.2	3.4	746	3.41
12:00	1705	34.8	8.09	2197.7	23.8	6.7	7.67	8.14	2199.6	24.4	7.8	0.8	756	3.70
13:00	1468	34.8	8.09	2200.1	24.0	6.6	7.50	8.16	2195.7	24.4	7.5	0.3	546	3.86
14:00	1702	34.8	8.10	2202.2	24.0	6.7	7.67	8.16	2194.7	24.6	7.8	1.6	534	3.93
15:00	1001	34.9	8.08	2194.6	24.1	6.7	7.83	8.15	2196.6	24.2	7.6	0.7	504	3.89
16:00	739	34.9	8.09	2208.4	24.1	6.6	7.67	8.15	2199.3	24.1	7.5	1.0	488	3.83
17:00	429	34.9	8.08	2208.1	24.0	6.4	7.67	8.12	2209.3	23.9	6.9	1.1	379	3.72
18:00	159	34.8	8.08	2210.7	23.9	6.3	7.67	8.08	2211.4	23.9	6.3	−0.3	127	3.49
19:00	32	34.9	8.07	2199.0	23.9	6.3	7.50	8.08	2203.3	23.5	6.2	−0.7	−50	3.34
20:00	0	34.9	8.07	2184.7	23.8	6.3	7.67	8.07	2189.4	23.5	6.0	−1.2	−135	3.28
21:00	0	34.9	8.07	2206.4	23.8	6.3	7.67	8.05	2203.0	23.5	6.0	−0.2	−179	3.18
22:00	0	34.9	8.04	2180.8	23.5	6.1	7.67	8.04	2199.1	23.3	6.0	−2.1	−147	3.10
23:00	0	34.9	8.01	2192.5	23.4	6.1	7.67	8.03	2199.4	23.3	5.9	−3.5	−87	3.05
0:00	0	34.9	8.06	2201.4	23.6	6.3	7.67	8.02	2199.2	23.3	6.0	−0.6	−124	2.99
1:00	0	35.0	8.04	2201.4	23.4	6.4	7.67	8.04	2201.2	23.2	5.8	0.3	−252	3.02
2:00	0	34.9	8.09	2214.8	23.7	6.3	7.67	8.06	2207.7	23.3	5.6	1.0	−344	3.13
3:00	0	34.9	8.06	2214.3	23.6	6.1	7.50	8.05	2207.0	23.1	5.8	2.0	−280	3.16
4:00	0	34.9	8.02	2209.2	23.3	6.2	7.50	8.04	2209.3	23.1	5.9	1.0	−169	3.10
5:00	0	34.9	8.10	2216.6	23.6	6.3	7.50	8.06	2211.6	23.4	5.8	0.7	−212	3.14
6:00	0	34.9	8.09	2214.3	23.5	6.1	7.50	8.07	2209.6	23.3	5.8	1.3	−216	3.23

Table 2 (*continued*)

Time	Outlet coral plus Algae mesocosm								Outlet coral only mesocosm							
	Flow liters min⁻¹	pH	A_T	Temp °C	O₂ Out mg l⁻¹	G_{net}	P_{net}	Mean Ω_{arag}	Flow liters min⁻¹	pH	A_T	Temp °C	O₂ Out mg l⁻¹	G_{net}	P_{net}	Mean Ω_{arag}
6:00	7.50	7.89	2190.8	23.0	5.6				8.33	7.93	2181.6	23.0	5.9			
7:00	7.50	7.92	2179.7	23.1	5.8	3.3	−264	2.36	8.33	7.89	2179.1	23.1	6.0	4.6	−59	2.38
8:00	7.50	7.97	2174.0	23.3	6.3	6.1	−67	2.55	8.00	7.96	2171.9	23.2	6.3	6.5	65	2.45
9:00	7.33	8.03	2165.2	23.4	7.5	6.2	361	2.83	8.17	7.99	2170.1	23.3	7.2	5.8	327	2.69
10:00	7.50	8.08	2156.9	23.5	8.9	8.5	883	3.12	8.33	8.04	2154.7	23.8	8.0	8.1	553	2.92
11:00	8.17	8.14	2165.3	24.3	8.4	11.6	956	3.49	8.17	8.10	2167.7	24.3	7.8	11.5	650	3.27
12:00	7.33	8.16	2165.7	24.5	8.4	10.2	983	3.80	8.00	8.12	2162.6	24.5	7.9	10.3	685	3.55
13:00	7.67	8.17	2162.9	24.4	8.1	9.3	853	3.89	8.33	8.13	2157.9	24.4	7.5	10.4	582	3.64
14:00	7.67	8.17	2159.3	24.6	8.4	10.8	845	3.93	8.33	8.12	2159.0	24.6	7.7	11.5	521	3.64
15:00	8.00	8.16	2164.4	24.3	8.1	9.5	768	3.89	8.67	8.10	2158.6	24.3	7.5	10.2	466	3.54
16:00	7.83	8.14	2174.3	24.0	7.8	9.0	644	3.77	8.00	8.09	2169.1	24.0	7.5	10.5	477	3.43
17:00	7.50	8.11	2183.0	23.9	7.0	8.3	472	3.61	8.00	8.09	2176.9	23.9	6.7	9.9	347	3.39
18:00	7.33	8.08	2194.5	23.6	6.2	5.6	61	3.43	8.33	8.06	2190.2	23.6	6.3	6.9	71	3.30
19:00	7.33	8.04	2190.3	23.6	5.9	3.4	−277	3.21	8.17	8.05	2187.2	23.5	6.0	4.4	−123	3.17
20:00	7.33	8.03	2172.5	23.2	5.9	2.9	−366	3.04	8.17	8.04	2177.7	23.3	6.0	2.6	−183	3.09
21:00	7.33	8.03	2192.6	23.2	5.6	3.6	−450	2.99	8.17	8.04	2192.5	23.2	5.8	2.9	−247	3.05
22:00	7.50	8.03	2189.4	23.2	5.6	0.7	−484	3.00	7.83	8.03	2185.6	23.3	5.7	1.3	−292	3.03
23:00	7.50	8.01	2190.4	23.1	5.6	−0.9	−410	2.94	8.17	8.02	2189.5	23.2	5.7	−0.2	−221	2.98
0:00	7.67	7.99	2188.3	23.2	5.6	2.0	−446	2.84	8.33	8.00	2188.6	23.2	5.8	2.1	−242	2.89
1:00	7.33	8.01	2190.2	23.2	5.4	3.3	−621	2.84	8.17	8.01	2190.2	23.2	5.6	3.3	−373	2.87
2:00	7.67	8.03	2196.5	23.3	5.2	4.0	−691	2.96	8.33	8.03	2194.1	23.2	5.4	4.3	−462	2.95
3:00	7.50	8.03	2197.2	23.2	5.3	4.9	−651	3.02	8.17	8.03	2195.7	23.2	5.6	5.4	−394	3.01
4:00	7.50	8.02	2200.2	23.1	5.4	3.6	−556	2.98	8.17	8.02	2199.3	23.1	5.7	3.9	−297	2.98
5:00	7.50	8.03	2200.5	23.4	5.4	3.4	−578	2.99	8.17	8.05	2199.1	23.2	5.6	3.8	−328	3.04
6:00	7.83	8.02	2200.3	23.3	5.4	4.0	−538	3.00	8.33	8.04	2199.1	23.2	5.7	4.4	−295	3.10
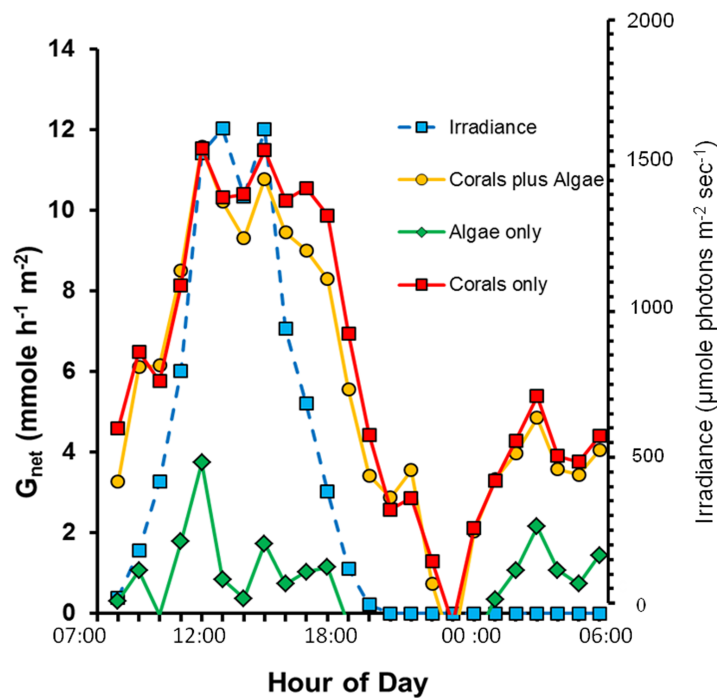
Figure 1 Diurnal net calcification rate (G_{net}) and irradiance for the three mesocosms.

night. There is a drop in calcification to zero around midnight with a dark calcification rate peak at approximately 03:00 h.

The relationship between G_{net} and Ω_{arag}

The linear regression of G_{net} plotted as a function of Ω_{arag} (Fig. 2) has become a widespread method of describing coral and coral reef calcification. A significant statistical relationship is obtained, with substantial variance that is generally assumed to be largely sampling error, or the result of other factors which influence G_{net}. However, the explanation appears be more complex, as will be discussed in the following sections.

Diel hysteresis, phase lags and night calcification patterns

McMahon et al. (2013) quantified G_{net} in a healthy coral reef lagoon in the Great Barrier Reef during different times of day. Their observations revealed a diel hysteresis pattern in the G_{net} versus Ω_{arag} relationship. This phenomenon can be demonstrated by labeling the points in Fig. 2 with the hour of day as shown in Fig. 3. The diel pattern moves from the lower left quadrant early in the day toward the upper right through mid-day and then back to the lower center during the night before returning to the lower left quadrant at first light. The pattern is nearly identical for the "Corals only" mesocosm (Fig. 3A) and the "Corals plus Algae" (Fig. 3B), which tracked each other closely (Fig. 1). The "Algae only" mesocosm did not show this pattern. The linear regression for the G_{net} vs. Ω_{arag} data for the mesocosm with coral (Fig. 2) accounted for part of the variance ($R^2 = 0.40$). A linear regression does not adequately describe the variance resulting from the diel pattern.

PeerJ
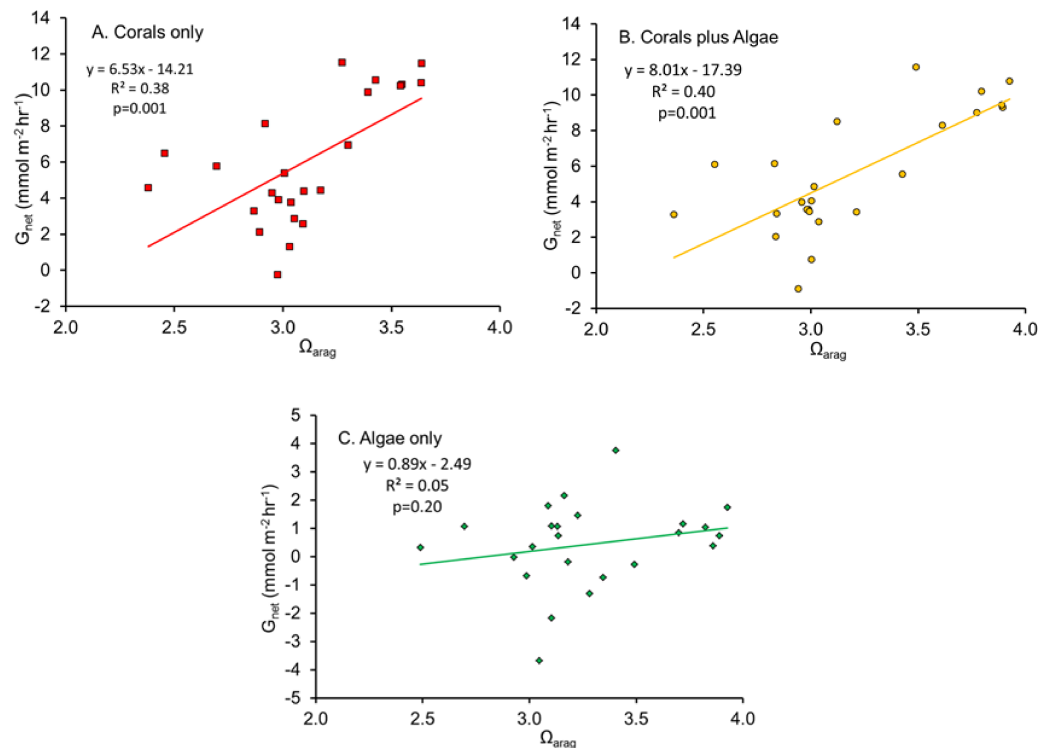
Figure 2 Net calcification rate (G_{net}) plotted as a function of Ω_{arag} for (A) "Coral only" mesocosm, (B) "Coral and Algae" mesocosm and (C) "Algae only" mesocosm.

Cyronak et al. (2013) used chambers to measure *in situ* benthic solute fluxes at three different advection rates at Heron Island lagoon, Australia and observed a strong diurnal hysteresis pattern similar to that in Fig. 3. They suggested that diel hysteresis is caused by the diurnal interaction between photosynthesis and respiration. The data did not follow a trend consistent with the Ω_{arag} of the water column being the main driver of carbonate precipitation and dissolution. Instead, carbonate precipitation and dissolution in these sediment communities is linearly correlated to the rates of photosynthesis and respiration (P_{net}) occurring over the same time period.

Phase shifts

Evaluation of phase relations for the various parameters listed in Table 2 can be facilitated by scaling each variable on a 0 to 1 scale. The normalized value of a_i for variable A in the ith row was calculated using the equation:

$$\text{Normalized value } (a_i) = \frac{a_i - A_{min}}{A_{max} - A_{min}} \tag{13}$$

where A_{min} is the minimum value for variable A and A_{max} is the maximum value for variable. Figure 4 summarizes the results for the variables most often considered in the literature (pH, Ω_{arag}, P_{net} and G_{net}).
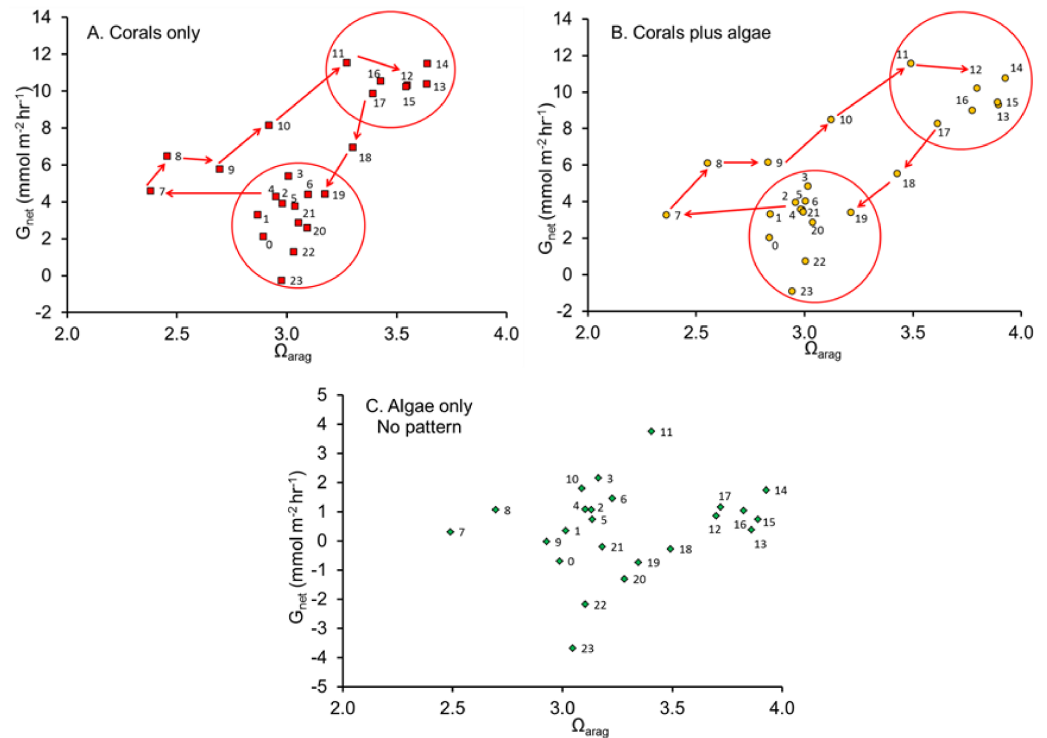
Figure 3 Net calcification rate versus Ω_{arag}. Net calcification rate versus Ω_{arag} with each point labeled with hour of the day revealing the clockwise coral reef diel hysteresis pattern for: (A) "Coral only" mesocosm, (B) "Coral plus Algae" mesocosm and the (C) "Algae only" mesocosm, which showed no pattern.

Figure 4 shows that peak pH and Ω_{arag} lag behind G_{net} throughout the daily cycle by two or more hours. The figure also shows that peak G_{net} follows P_{net} during daylight photosynthetic hours with a reverse during the nighttime hours. *Shamberger et al. (2011)* reported that Ω_{arag} lags behind G_{net} on the reefs of Kaneohe Bay, Hawaii. *McMahon et al. (2013)* reported that peak G_{net} rates occurred 2–3 h before the Ω_{arag} maximum on a healthy coral reef on the Great Barrier Reef. Thus Ω_{arag} (along with closely correlated $[CO_3^{2-}]$, pH and [DIC]:[H$^+$] ratio) is not the primary driver of coral calcification over a diurnal cycle. The paradigm that Ω_{arag} correlates with G_{net} on a global scale must be tempered with the caveat that other processes have a much greater influence on calcification on smaller spatial and temporal scales. The data presented above show that diurnal irradiance drives P_{net}, which in turn drives G_{net}, and which alters pH, which controls $[CO_3^{2-}]$ and Ω_{arag} as well as other variables based on concentration such as the ratio of [DIC] to [H$^+$]. A better understanding of this hierarchy will resolve many of the contradictions in the literature on coral reef calcification.

Night calcification

Laboratory studies show that coral calcification continues in darkness, but at a lower rate than observed in light enhanced calcification (*Schneider & Erez, 2006*). Night calcification rates have generally been assumed to be low and constant at night, although this assump-
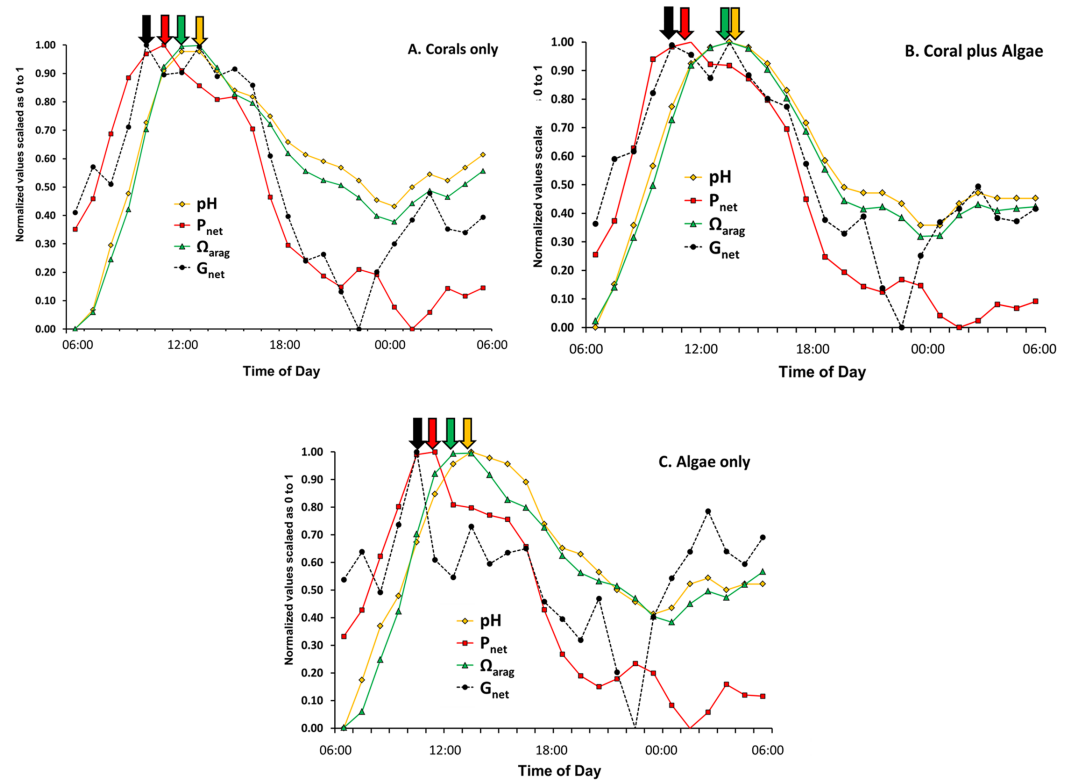
Figure 4 Normalized pH, Ω_{arag}, P_{net} and G_{net} values for the three mesocosms versus time of day using data from Table 2 and Eq. (9). Arrows point to relative maxima for each parameter.

tion has largely gone untested. Figures 1 and 4 show decreasing dark calcification following sunset, reaching zero near midnight followed by an increasing rate of dark calcification and an increase in respiration (Figs. 5C and 5D) that rises to a peak at 03:00 well before dawn. This pattern has occurred consistently in our mesocosm experiments, with the same pattern observed in 30 separate mesocosm runs with different communities under various conditions as well as in flume studies at our site (*Murillo, Jokiel & Atkinson, 2014*). *Barnes & Crossland (1980)* used time-lapse photography to measure diurnal growth in the staghorn coral *Acropora acuminata* and found that night-time extension rate was similar to or greater than day-time extension. They suggested that, "symbiotic association permits rapid growth because the coral can invest in flimsy scaffolding at night with the certainty that bricks and mortar will be available in the morning". *Wooldridge (2013)* has proposed a new model for "dark" coral calcification, whereby O_2-limitation of aerobic respiration during the night initiates a homeostatic host response that forms the skeletal organic matrix. The matrix formed at night subsequently allows rapid growth of the aragonite fibers during the "light-enhanced" period of calcification, when abundant energy derived from photosynthesis is available. Perhaps the mid-night calcification minimum observed in Figs. 1 and 4 at 00:00 reflects this period of organic matrix formation that precedes the 03:00 night calcification peak.
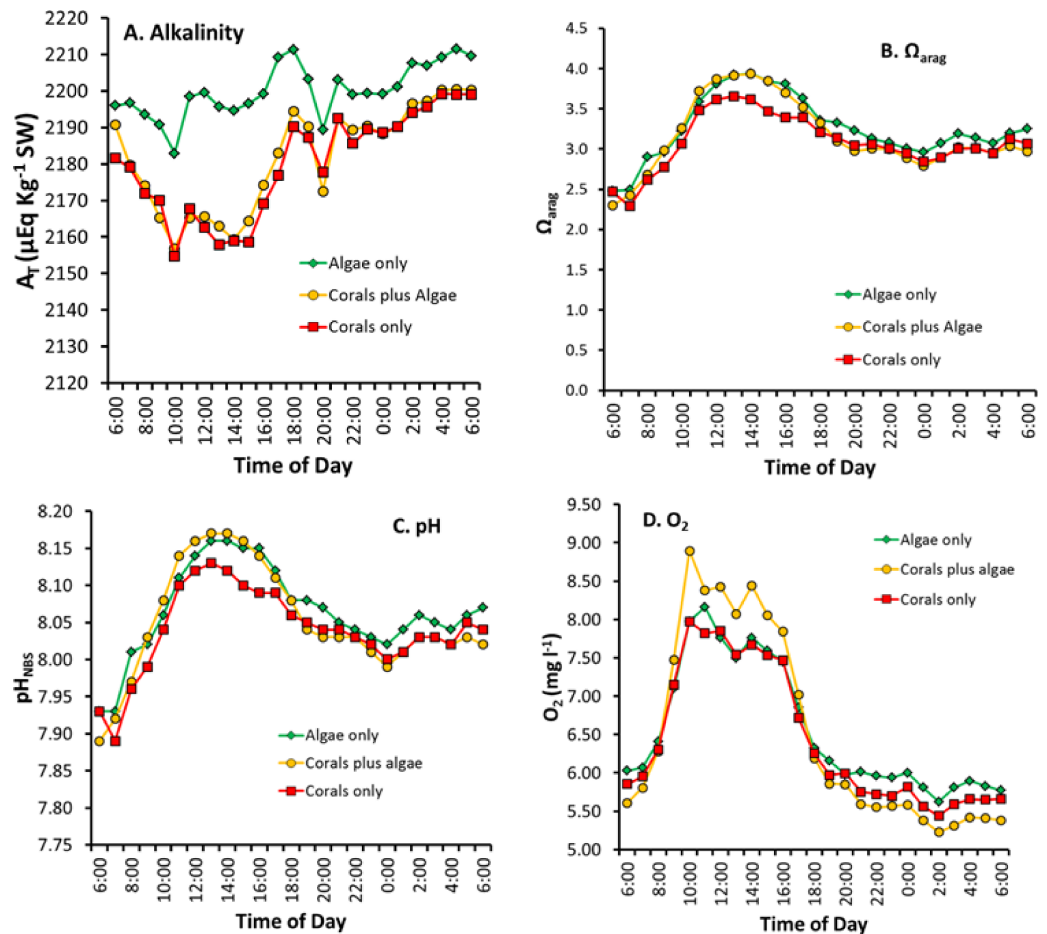
Figure 5 Diurnal changes in seawater chemistry in the three mesocosms for: (A) total alkalinity A_T, (B) aragonite saturation state Ω_{arag}, (C) pH and (D) dissolved oxygen.

Diurnal changes in concentration of A_T, pH, Ω_{arg} and DO

The variables of A_T, pH, Ω_{arg} DIC, and DO are concentrations while P_{net} and G_{net} are flux rates. Care must be taken when comparing concentrations to flux rates because flux rate can be high when concentration is high or low. Or flux rate can be low when concentration is high or low. Figure 4 shows patterns that are difficult to interpret because the figure mixes flux rates with concentrations. This issue will be discussed and resolved later in this discussion, but first we will compare differences in concentrations of key variables over the diurnal cycle (Fig. 5).

Figure 5 reveals several important patterns:

1. Alkalinity in the "Algae only" mesocosm remained high during the entire diurnal cycle. In contrast, the mesocosms containing corals showed lower A_T (Fig. 5A) caused by rapid calcification. A_T reduction by the corals was greatest during the daylight hours when G_{net} was high (Fig. 1) with the difference diminishing during nighttime hours.
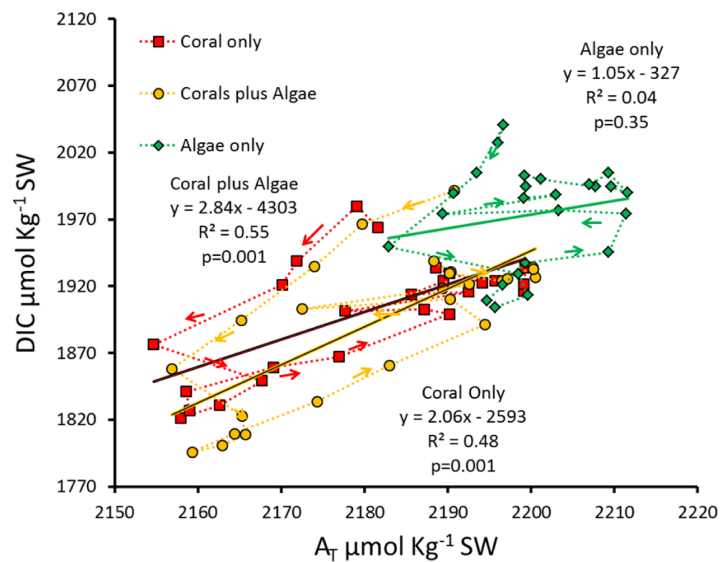
Figure 6 Hourly DIC versus A_T for the diurnal data measured in each of the three mesocosms. Successive hours are connected by the dotted lines to show the patterns of diurnal hysteresis.

2. The two mesocosms with algae maintained a higher Ω_{arag} throughout the mid-day portion of the diurnal cycle (Fig. 5B) which can be attributed to higher pH resulting from rapid rates of algae photosynthesis and coral photosynthesis (Eqs. (6)–(8)), with a less pronounced difference during the rest of the cycle.

3. The extreme difference in Ω_{arag} between the "Corals only" and the "Corals plus Algae" mesocosms (Fig. 5B) did not produce a corresponding difference in G_{net} between the two mesocosms (Fig. 1), which demonstrates that Ω_{arag} is uncoupled from G_{net} and explains differences encountered when comparing the Ω_{arag} versus G_{net} relationship in different systems with different diurnal P_{net} regimes.

4. Night-time pH and Ω_{arag} values (Figs. 5B and 5C) show less variability than G_{net} (Fig. 1).

5. The high biomass in the "Coral plus Algae" mesocosm (Fig. 5D) resulted in the highest O_2 values during daylight hours (due to photosynthesis) and the lowest O_2 during the night (due to respiration). The "Algae only" treatment had the second highest daytime level O_2 due to algal photosynthesis and relatively high levels of O_2 at night.

6. The 03:00 calcification peak observed in Fig. 1 is shown by both a decrease in O_2 concentration and a drop in pH due to accelerated respiration. DO (Fig. 5D) and the pH (Fig. 5C) are measured independently and both show this effect to corroborate the observation.

Plotting DIC versus A_T (Fig. 6) demonstrates the major influence of P_{net} on seawater Ω_{arag}. Calcification and dissolution shift A_T values horizontally along the abscissa in Fig. 6 and influence DIC values vertically along the ordinate. However, photosynthesis and respiration change DIC along the ordinate without changing A_T. The observed hysteresis

PeerJ ____

pattern results from P_{net} driving G_{net} and increasing pH. A linear relationship accounting for only half of the variance ($R^2 \approx 0.5$) between DIC and A_T was observed for the two rapidly calcifying mesocosms containing corals. This relationship does not hold for the low-calcification "Algae only" mesocosm.

As pointed out by *McMahon et al. (2013)*, connecting the points on a graph of A_T vs. DIC reveals a circular hysteresis pattern over the diel cycle as shown for the G_{net} versus Ω_{arag} plot (Fig. 6). G_{net} can account for changes in both the A_T and DIC concentrations. However, P_{net} can only account for changes DIC concentration. Therefore, Ω_{arag} is a function of the changes in carbonate chemistry due to both P_{net} and G_{net}, and any changes in DIC concentration relative to A_T will result in different influences on Ω_{arag}. For example, in systems with high organic production relative to calcification (Coral plus Algae mesocosm), Ω_{arag} will increase during daylight due to high pH caused by high uptake of CO_2 used for photosynthesis (Fig. 5D). Conversely, in systems with low organic production relative to calcification (Coral only mesocosm), Ω_{arag} will decrease due to the uptake of A_T. Any decrease in G_{net} associated with an increase in P_{net} will increase Ω_{arag} and change the way that G_{net} responds to OA. Therefore, any prediction of future global changes on coral reef G_{net} based on oceanic seawater Ω_{arag} must also take into account the influence of future localized P_{net} on G_{net} and Ω_{arag} as well as changes in carbonate dissolution of reef carbonates as described by *Murillo, Jokiel & Atkinson (2014)* for each reef location.

Comparisons between the hourly and daily G_{net} and P_{net} values (Table 3) show a similar calcification rate for both the "Coral only" mesocosm and the "Coral plus Algae" mesocosm in spite of the differences in DO, pH, A_T (Fig. 5) and P_{net}. However, daily P_{net} for the "Coral plus Algae" mesocosm was only one third of the P_{net} of the "Coral only" mesocosm. Hourly production was much higher in the "Corals plus Algae" mesocosm during the daylight hours, but production was consumed by extremely high respiration during nighttime hours. The "Algae only" mesocosm showed very low daily G_{net} and extremely high daily P_{net}.

Anthony, Kleypas & Gattuso (2011) proposed a model that areas dominated by algal beds draw CO_2 down and elevate Ω_{arag}, potentially offsetting ocean acidification impacts at the local scale. Their model is based on the paradigm that G_{net} is controlled by Ω_{arag}. Results suggested that a shift from coral to algal abundance under ocean acidification can lead to improved conditions for calcification (i.g. increased Ω_{arag}) in downstream habitats and that alga beds can provide a significant mechanism for buffering ocean acidification impacts at the scale of habitat to reef. However, this conclusion is at odds with the measured values shown in Table 3 and Fig. 5. G_{net} in the "Corals plus Algae" treatment was the same as the "Coral Only" treatment even though the Ω_{arag} was much higher. In addition, the presence of the algae caused a precipitous drop in P_{net}. The flaw in their model appears to be the assumption that G_{net} is controlled by Ω_{arag}. Algal photosynthesis increases pH which shifts the equilibrium to higher $[CO_3^{2-}]$ and thus higher Ω_{arag}. There is a direct correlation between G_{net} and Ω_{arag} for a specific reef community, but not a cause and effect relationship.
Table 3 Hourly and daily G_{net} and P_{net} values for the three mesocosms.

Time of day	Solar irradiance µmol photons m^{-2} s^{-1}	G_{net} (mmol m^{-2} h^{-1})			P_{net} (mmol m^{-2} h^{-1})		
		Corals only	Corals plus Algae	Algae only	Corals only	Corals plus Algae	Algae only
07:00	56.3	4.6	3.3	0.3	−59	−264	22
08:00	221.6	6.5	6.1	1.0	65	−67	127
09:00	464.6	5.8	6.2	0.0	327	361	340
10:00	854.0	8.1	8.5	1.6	553	883	539
11:00	1619.0	11.5	11.6	3.4	650	956	746
12:00	1705.0	10.3	10.2	0.8	685	983	756
13:00	1468.0	10.4	9.3	0.3	582	853	546
14:00	1702.0	11.5	10.8	1.6	521	845	534
15:00	1001.0	10.2	9.5	0.7	466	768	504
16:00	739.0	10.5	9.0	1.0	477	644	488
17:00	429.0	9.9	8.3	1.1	347	472	379
18:00	159.0	6.9	5.6	−0.3	71	61	127
19:00	31.7	4.4	3.4	−0.7	−123	−277	−50
20:00	0.0	2.6	2.9	−1.2	−183	−366	−135
21:00	0.0	2.9	3.6	−0.2	−247	−450	−179
22:00	0.0	1.3	0.7	−2.1	−292	−484	−147
23:00	0.0	−0.2	−0.9	−3.5	−221	−410	−87
24:00	0.0	2.1	2.0	−0.6	−242	−446	−124
01:00	0.0	3.3	3.3	0.3	−373	−621	−252
02:00	0.0	4.3	4.0	1.0	−462	−691	−344
03:00	0.0	5.4	4.9	2.0	−394	−651	−280
04:00	0.0	3.9	3.6	1.0	−297	−556	−169
05:00	0.0	3.8	3.4	0.7	−328	−578	−212
06:00	0.0	4.4	4.0	1.3	−295	−538	−216
Daily (mmol m^{-2} d^{-1})		144	133	10	1226	427	2913

Diurnal changes in material flux (P_{net}, G_{net}, H$^+$ flux and DIC flux)

G_{net} and P_{net} are measures of material flux. DO, pH and DIC are measures of concentration. The preceding discussion and numerous publications often compare concentrations of one material to flux rate of another material or vice versa. Much more can be learned by plotting DIC flux and H$^+$ flux rather than [DIC], [H$^+$] or pH in relation to P_{net} and G_{net}. DIC flux and H$^+$ flux were calculated using the box model and graphed on a 0 to 1 scale in the same manner as in Fig. 4 with the result presented as Fig. 7. This figure illustrates the dynamic geochemical and physiological relationships involved in coral and coral reef metabolism.

DIC flux (uptake) in the highly calcifying mesocosms containing coral (Fig. 7) increases with increasing P_{net} from 06:00 until mid-day peak P_{net} and then decreases rapidly as P_{net} decreases with decreasing irradiance. *Furla et al. (2000)* demonstrated the presence of a DIC pool within coral tissues. The size of this pool was dependent on the lighting
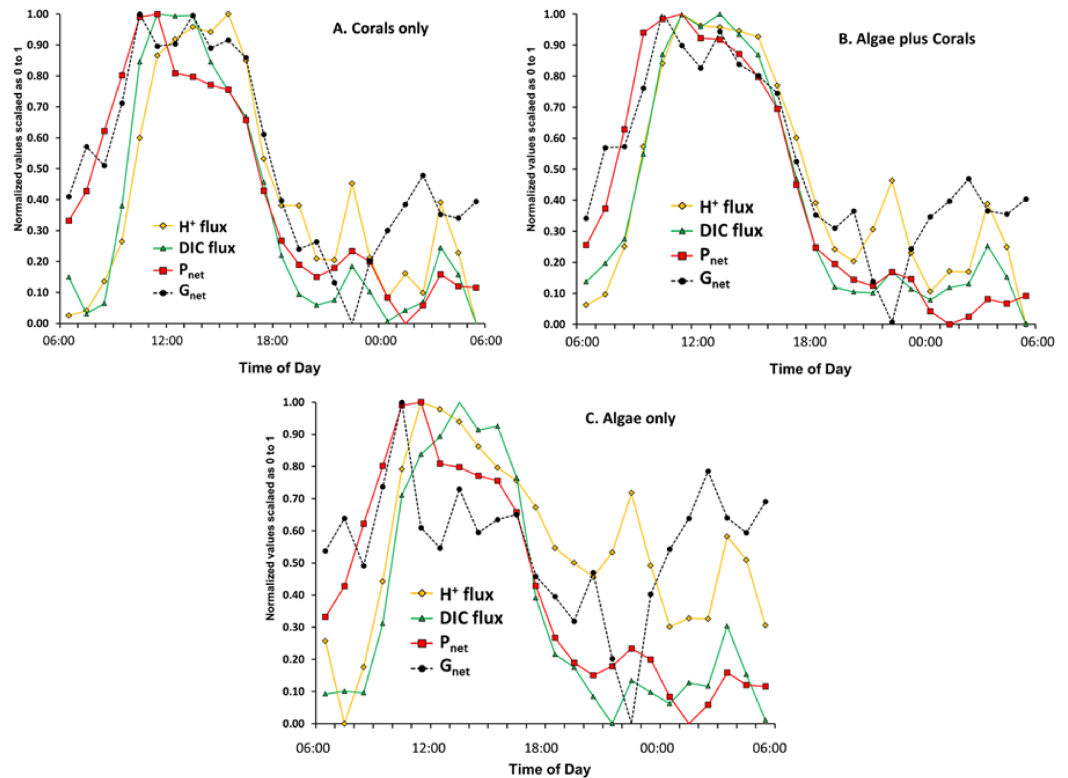
Figure 7 Plot of normalized data for P_{net}, G_{net}, inverse DIC flux and H$^+$ flux for the experiment.

conditions, since it increased 39-fold after 3 h of illumination. If we apply this observation to the data shown in Fig. 7, it appears that the DIC pool had increased by mid-day, so rate of DIC uptake dropped rapidly as irradiance and photosynthesis declined. However, note that the high dissipation rates of H$^+$ continued for 2–3 h following the peak rates of P_{net} and G_{net} as the corals rid themselves of the backlog of H$^+$ generated by rapid calcification. Thus the lag of pH behind the peak flux rates of P_{net} and G_{net} (Figs. 4A and 4B) represents a disequilibrium that results from the lag in proton efflux from the corals. The correlation between Ω_{arag} and G_{net} is simply the response of the CO$_2$-carbonate system to pH as [H$^+$] shifts the equilibria and redistributes the [CO$_3^{2-}$] relative to the other DIC components of [HCO$_3^-$] and [CO$_2$] (Eqs. (3)–(5)) . Therefore Ω_{arag} closely tracks pH whereas G_{net} tracks P_{net} more closely. Changes in Ω_{arag} are a consequence of changes in P_{net} and G_{net}, rather than a driver of G_{net}. Hence the Ω_{arag} peak and the pH peak lag behind the P_{net} and G_{net} peaks (Figs. 4A and 4B) due to lag in proton efflux seen in Fig. 7. This observation demonstrates the importance of understanding the difference between H$^+$ concentration and H$^+$ flux.

During the night the H$^+$ flux rate is very responsive to changes in G_{net} in the "Algae only" and "Coral plus Algae" due to large changes in respiration (Fig. 7). The fluctuations of proton flux at night in the "Coral only" mesocosm are dampened considerably compared to the "Algae only" treatment. The "Coral plus Algae" mesocosm shows an intermediate response. Perhaps the coral skeleton acts as a buffer in a manner similar
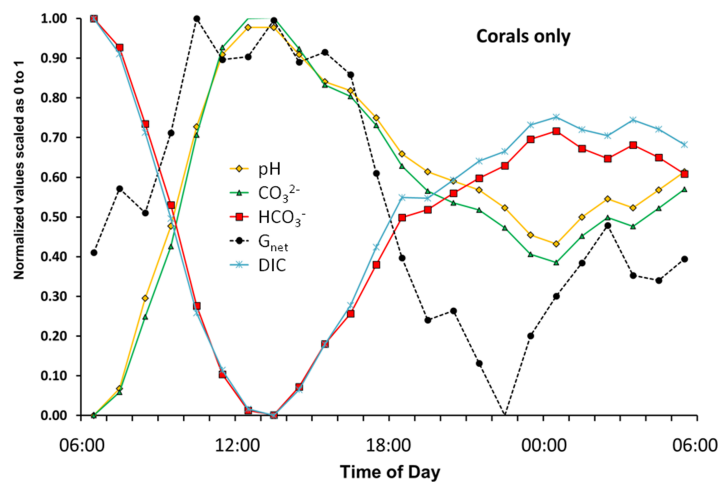
Figure 8 The flux rate of calcification-dissolution (G_{net}) plotted against the concentrations of important variables of the CO_2-carbonate system for the "Corals only" mesocosm.

to that proposed by *Suzuki, Nakamori & Kayanne (1995)*. The macroalgae lack the large skeletal carbonate buffer of reef corals.

Back to the basics

The preceding sections have established the importance of using flux rates rather than concentrations when we are describing a dynamic metabolic system such as a coral or coral reef. Most of the previous research in this area has focused on the relationship between G_{net}, $[CO_3^{2-}]$ (or its surrogate Ω_{arag}), $[HCO_3^-]$, and $[H^+]$ expressed as pH. Plotting these variables in exemplary Fig. 8 is very informative and sheds light on results of previous studies.

A coral must uptake inorganic carbon in order to maintain photosynthesis and calcification. As a result [DIC] will decrease no matter which carbonate species (HCO_3^-, CO_3^{2-} or CO_2) is taken up by the coral (Eqs. (3)–(5)). Thus we see a decline in [DIC] at high rates of G_{net} (Fig. 8). $[HCO_3^-]$, which has been identified as the preferred substrate for photosynthesis and calcification (*Weis, Smith & Muscatine, 1989*; *Furla et al., 2000*; *Roleda, Boyd & Hurd, 2012*) closely tracks [DIC] during daylight hours. In contrast, $[CO_3^{2-}]$ lags behind G_{net} and closely tracks pH during the day as shown for Ω_{arag} in Fig. 4. If $[CO_3^{2-}]$ (or its surrogate Ω_{arag}) drives calcification, then how do we explain the lag behind G_{net}? And if $[CO_3^{2-}]$ is limiting, how do we explain the fact that $[CO_3^{2-}]$ is increasing rather than decreasing as the coral calcifies rapidly and takes up inorganic carbon? $[CO_3^{2-}]$ increases because of the increase in pH caused by rapid photosynthesis, which shifts the equilibrium between $[HCO_3^-]$ and $[CO_3^{2-}]$. Thus, P_{net} is the driver of changes in G_{net} and $[CO_3^{2-}]$ (Eqs. (2)–(5)). A basic physiological interpretation of the patterns shown in Fig. 8 is that daytime coral metabolism rapidly removes DIC (primarily in the form of HCO_3^-) while photosynthesis provides the energy that drives G_{net} (Fig. 4). Higher pH resulting from rapid photosynthesis pushes the equilibria toward higher $[CO_3^{2-}]$. This scenario results in a correlation between G_{net} and Ω_{arag}, with Ω_{arag} as the dependent variable.

During the night $[HCO_3^-]$, $[DIC]$, $[CO_3^{2-}]$ and pH mirror changes in G_{net}. However, note that $[HCO_3^-]$ diverges from $[DIC]$ and $[CO_3^{2-}]$ diverges from pH in darkness. The night divergence can be attributed to respiration causing a decrease in pH. The decreasing pH shifts the equilibria so that $[CO_3^{2-}]$ is converted to $[HCO_3^-]$, thereby changing the offset between the points. This phenomenon is also reflected in the pattern of diurnal hysteresis show in Fig. 3.

CONCLUSIONS AND RECOMMENDATIONS

Correlations do not establish cause and effect

Linear regression using Ω_{arag} as the independent variable may be useful as a first approximation, but is a poor descriptor of calcification dynamics on coral reefs. Much of the existing data on coral calcification was developed in static or low turnover incubation experiments under typical laboratory low irradiance artificial light sources on a 12 h light, 12 h dark cycle (*Jokiel, Bahr & Rodgers, in press*). This regime results in an unrealistic simulation of the actual diurnal cycle that occurs on coral reefs. The standard protocol has been to compare linear regressions between or among treatments. Linear regression provides a very limited description of the actual relationship between the key factors controlling organic and inorganic processes on coral reefs, which are more adequately described by data presentations such as that in Table 3 or Fig. 7. The linear regression approach does not fully embrace natural diurnal calcification patterns and phase lags because these processes are non-linear. The linear regression approach can lead to the assumption that Ω_{arag} is the independent variable driving the calcification reaction. Nevertheless, correlations at a single location or in a single experiment can result where all other factors are held constant because the two quantities are related to some extent. Use of Ω_{arag} as an independent variable to compare spatial and temporal variation in G_{net} is known to create difficulties (*Shamberger et al., 2011*; *Falter et al., 2012*).

Numerous field and laboratory studies have demonstrated a positive correlation between G_{net} and Ω_{arag} for corals and coral reefs *Erez et al. (2011)*. Well-developed reefs occur within a narrow geographic range characterized by open ocean $\Omega_{arag} > 3.3$ (*Kleypas et al., 1999*), which could mean that coral communities have limited capacity to adapt to future levels of anthropomorphic ocean acidification (OA) projected for the 21st century. Recent reports suggest that healthy coral reefs could cease to exist within this time frame as OA continues and oceanic Ω_{arag} decreases (*Hoegh-Guldberg et al., 2007*; *Silverman et al., 2009*). However, there are inconsistencies in the relationship (slope and *x*-intercept) between G_{net} as a function of Ω_{arag} on various reefs throughout the world (*Shamberger et al., 2011*). For example, Kaneohe Bay, Oahu, Hawaii contains rich coral reefs that show extremely high rates of G_{net} while living at low Ω_{arag} levels (mean $\Omega_{arag} = 2.85$) (*Shamberger et al., 2011*). *Shamberger et al. (2014)* report the existence of highly diverse, coral-dominated reef communities at the Rock Islands of Palau that are living at low saturation states ($\Omega_{arag} = 1.9–2.5$). These values approach those projected for the tropical western Pacific open ocean by 2100 under future OA modeling scenarios. Identification of biological and environmental factors that enable these communities to persist at low Ω_{arag}

could provide important insights into the future of coral reefs under increasing OA. So how do we account for the paradox of rich coral reefs growing at low Ω_{arag}? Previous work has been based on the assumption that G_{net} is controlled by or related directly to Ω_{arag}. The present investigation indicates that P_{net} rather than Ω_{arag} drives G_{net} and that calcification rate is further limited by proton flux, with pH and A_T playing the major role in controlling calcification. Ω_{arag} on coral reefs is simply a dependent variable being controlled largely by changes in pH due to photosynthesis. A correlation will exist at a given site, but will not be consistent between different coral reef communities.

The [DIC]:[H$^+$] ratio correlates with Ω_{arag} in describing G_{net} and is useful from a physiological point of view because it involves pH and all of the inorganic carbon species (*Jokiel, 2011a*; *Jokiel, 2013*). However, the [DIC]:[H$^+$] ratio is simply another variable based on concentration (along with pH, Ω_{arag}, CO_3^{2-}, etc.) that shows a correlation with G_{net}. Nevertheless, the [DIC]:[H$^+$] ratio can be important in describing G_{net} in situations where Ω_{arag} is decoupled from [H$^+$] as occurs in the paleo-ocean over time scales greater than 10,000 years (*Hönisch et al., 2012*). A calcifying organism must uptake DIC in order to continue the calcification reaction and must rid itself of the waste protons. So G_{net} correlates directly to [DIC] and inversely to [H$^+$].

Results of this investigation (Fig. 7) demonstrate the difficulty that corals encounter in shedding waste protons generated during calcification. High rates of H$^+$ flux continued for several hours following peak G_{net}. An important conclusion of this work is that measurements of DIC flux and H$^+$ flux are far more useful in describing coral metabolism dynamics than [DIC] and [H$^+$] (Fig. 8). Likewise, Ω_{arag} is not a very useful variable in that it simply tracks pH (Fig. 4). This pattern becomes clear when one considers that [CO_3^{2-}] (and hence Ω_{arag}) shifts with changing [H$^+$] as described in Eqs. (2)–(5). DIC flux follows P_{net} and G_{net} and decreases rapidly following peak P_{net} and peak G_{net} indicating that corals can cope more effectively with the problem of DIC supply compared to the problem of eliminating H$^+$.

Future research directions

The time lag between G_{net} and Ω_{arag} reported previously in field studies (*Shamberger et al., 2011*; *Cyronak et al., 2013*; *McMahon et al., 2013*) provides evidence that diffusion and advection of materials between the coral and the water column involves time delays. One reason is that corals convert inorganic carbon to organic carbon, translocate the organic carbon to distal calcification sites, store organic carbon as lipid, and can eventually convert stored organic carbon back to inorganic carbon (*Jokiel, 2011b*), creating numerous possible phase lags for metabolic materials. The second reason for the time lag is that rapidly calcifying systems have difficulty dissipating waste protons as shown by continued rapid proton efflux for hours after peak calcification (Fig. 7). What other mechanisms can account for the phase lag? Boundary layers (BL) can slow the exchange of metabolic materials between the coral and the water column. The results of *Cyronak et al. (2013)* revealed that stirring had a net stimulatory effect on A_T flux and on the diurnal cycle

of hysteresis. Boundary layers slow exchange of metabolic materials, so this is an area of investigation that can provide an explanation.

Three hydrodynamic boundary layers have previously been defined and measured (*Shashar, Cohen & Loya, 1993*; *Shashar et al., 1996*). The Diffusion Boundary Layer (DBL) is only a few mm thick and in contact with the coral epidermis. The Momentum Boundary Layer (MBL) controls water movement in the proximity of the sessile organisms and is thicker by an order of magnitude than the DBL. The Benthic Boundary Layer (BBL), which controls the interactions of the reef with the surrounding sea water, was typically found to be more than 1 m thick and characterized by a roughness height of 31 cm and a shear velocity of 0.42 cm s^{-1} in the studies.

The DBL is a thin layer of stagnant seawater adjacent to the coral produced by frictional drag. This quiescent layer influences the flux of material between the benthic surface and the water column. The transport of Ca^{2+}, CO_2, CO_3^{2-}, HCO_3^-, O_2, nutrients and H^+ through the DBL is limited by the physical processes of diffusion and advection (*Jokiel, 1978*; *Lesser et al., 1994*; *Kaandorp et al., 2005*; *Kaandorp, Filatov & Chindapol, 2011*). *Kühl et al. (1995)* found that zooxanthellae photosynthesis resulted in a build-up of O_2 in the photosynthetic tissue of up to 250% saturation and a tissue pH of up to 8.6 (i.e., 0.7 pH units above the pH value of the overlying seawater). In darkness the O_2 within the coral tissue was depleted by respiration to near anoxic (<2% air saturation) conditions, with tissue pH of 7.3–7.4. O_2 and pH profiles demonstrated the presence of a 200–300 μm thick DBL that separated the coral tissue from the overlying flowing seawater. Various models invoke boundary layer controls on coral metabolism. *Kaandorp et al. (2005)* and *Kaandorp, Filatov & Chindapol (2011)* addressed DBL limitation of DIC influx while *Jokiel (2011a)*, *Jokiel (2011b)* and *Jokiel (2013)* challenged the paradigm that calcification is limited by CO_3^{2-} supply on the reactant side of the calcification equation. Rather, he argued that rate of dissipation of H^+ on the product side due to boundary layer conditions can be the actual limiting factor.

Boundary layer limitation of photosynthesis provides an analog to boundary layer limitation of calcification. Photosynthetic rate can be limited by rate of waste O_2 dissipation through the boundary layer rather than being limited by supply of reactant CO_2. By analogy, calcification can be limited by rate of removal of waste protons rather than by availability of inorganic carbon. The importance of water motion in reducing boundary layer thickness and thereby increasing oxygen flux between the photosynthetic organisms and the water column has been demonstrated (*Mass et al., 2010*). By analogy, increased water motion can decrease boundary layer thickness and thereby increase removal of protons from the coral.

Studies of reef metabolism beginning with the classic work of *Odum & Odum (1955)* at Enewetak Reef flat and followed by others (*Shamberger et al., 2011*; *Falter et al., 2012*) were conducted in shallow water reef flats within the BBL in situations where unidirectional currents allowed calculation of flux rates. Substantial boundary layers occur over all reefs. For example, *Price et al. (2012)* investigated a range of sites from exposed coastal situations to lagoons and found that ambient variability in pH was substantial

and oscillated over a diurnal cycle with diel fluctuations in pH exceeding 0.2. Daily pH maxima were identified as an important control on calcification. Net accretion among sites was positively related to the magnitude and duration of pH above the climatological seasonal low, despite myriad other ecological (e.g., local supply, species interactions, etc.) and physical oceanographic (e.g., temperature, current magnitude and direction, wave strength, latitudinal gradients, etc.) drivers. In general, accretion rates were higher at sites that experienced a greater number of hours at high pH values each day. Where daily pH within the BBL failed to exceed pelagic climatological seasonal lows, net accretion was slower and fleshy, non-calcifying benthic organisms dominated space. Thus, key aspects of coral reef ecosystem structure and function are clearly related to natural diurnal variability in pH, which is driven primarily by photosynthesis and respiration as P_{net}.

The master variables

The practice of calculating and comparing linear regressions of G_{net} vs. Ω_{arag} to obtain a first approximation of calcification rates under different conditions is fraught with problems but probably will continue because it is ingrained in science and is convenient to use. The correlation of a primary biological response (G_{net}) to a primary physical chemistry measurement (Ω_{arag}) is attractive, especially in modeling the possible future changes on coral reefs. Unfortunately, the physical chemistry concept of Ω_{arag} has no basic physiological meaning in describing G_{net} other than a correlation with the [DIC]: [H$^+$] ratio (*Jokiel, 2013*) as well as with other factors such as pH. There is no consistent relationship between Ω_{arag} and G_{net} when comparing reefs throughout the world (*Shamberger et al., 2011*). Coral reefs are systems in constant disequilibrium with the water column. So we must take care not to be led astray in our thinking about the variables that actually drive and control coral and coral reef metabolism and bulk water chemistry. The correlation between G_{net} and other factors is a result of P_{net} driving both G_{net} and Ω_{arag} (*McMahon et al., 2013*). The observed phenomenon of diurnal hysteresis and diurnal phase lag show the importance of measuring flux rates and emphasizes the challenge in predicting the future effects of OA on coral reefs. The method of using linear extrapolations of Ω_{arag} to determine threshold levels that will shift coral reefs from net calcifying systems to a net dissolving state has been questioned (*McMahon et al., 2013*). Perhaps predicted changes in Ω_{arag} in the open ocean can be used to calculate changes on reefs if we assume that the baseline on the reefs will change in concert with ocean values and that all other processes such as P_{net} and carbonate dissolution will not be influenced by OA. An explanation for the many paradoxes of coral calcification discussed herein has been presented as the "Two Compartment Proton Flux Model of Coral Metabolism" (*Jokiel, 2011b*). This model is focused on localized gradients that influence coral metabolism with a focus on proton flux, carbon pools and translocation of fixed carbon. A major feature of the model is the presence of boundary layers which control local pH gradients and inorganic carbon speciation in addition to proton flux. Results of the present investigation support this model.

Funding

This work funded by the Pacific Island Climate Change Cooperative and the University of Hawaii. The funders had no role in study design, data collection and analysis, decision to publish, or preparation of the manuscript.

Grant Disclosures

The following grant information was disclosed by the authors:
Pacific Island Climate Change Cooperative.
University of Hawaii.

Competing Interests

The authors declare there are no competing interests.

Author Contributions

- Paul L. Jokiel conceived and designed the experiments, performed the experiments, analyzed the data, contributed reagents/materials/analysis tools, wrote the paper, prepared figures and/or tables, reviewed drafts of the paper.
- Christopher P. Jury analyzed the data, contributed reagents/materials/analysis tools, wrote the paper, reviewed drafts of the paper.
- Ku'ulei S. Rodgers performed the experiments, analyzed the data, contributed reagents/materials/analysis tools, wrote the paper, reviewed drafts of the paper.

REFERENCES

Andersson AJ, Kuffner IB, Mackenzie FT, Jokiel PL, Rodgers KS, Tan A. 2009. Net loss of $CaCO_3$ from coral reef communities due to human induced seawater acidification. *Biogeosciences Discussion* **6**:1–20.

Anthony KRN, Kleypas JA, Gattuso J-P. 2011. Coral reefs modify their seawater carbon chemistry–implications for impacts of ocean acidification. *Global Change Biology* **17**:3655–3666 DOI 10.1111/j.1365-2486.2011.02510.x.

Barnes DJ, Crossland CJ. 1980. Diurnal and seasonal variations in the growth of a staghorn coral measured by time-lapse photography. *Limnology & Oceanography* **35(6)**:1113–1117 DOI 10.4319/lo.1980.25.6.1113.

Cyronak T, Santos IR, McMahon A, Eyre BD. 2013. Carbon cycling hysteresis in permeable carbonate sands over a diel cycle: implications for ocean acidification. *Limnology & Oceanography* **58(1)**:131–143 DOI 10.4319/lo.2013.58.1.0131.

Dickson A, Millero FJ. 1987. A comparison of the equilibrium constants for the dissociation of carbonic acid in seawater media. *Deep-Sea Research* **38**:1733–1743 DOI 10.1016/0198-0149(87)90021-5.

Dickson A, Sabine CL, Christian JR (eds.) 2007. *Guide to best practices for ocean* CO_2 *measurements*, 3. PICES Special Publication, 191. *Available at http://cdiac.ornl.gov/ftp/oceans/ Handbook_2007/Guide_all_in_one.pdf.*

Erez J, Reynaud S, Silverman J, Schneider K, Allemand D. 2011. Coral calcification under ocean acidification and global change. In: Dubinsky Z, Stambler N, eds. *Coral reefs: an ecosystem in transition*. New York: Springer Press, 151–176.

Falter JL, Lowe RJ, Atkinson MJ, Cuet P. 2012. Seasonal coupling and de-coupling of net calcification rates from coral reef metabolism and carbonate chemistry at Ningaloo Reef, Western Australia. *Journal of Geophysical Research* **117**:C05003 DOI 10.1029/2011JC007268.

Furla P, Galgani I, Durand I, Allemand D. 2000. Sources and mechanisms of inorganic transport for coral calcification and photosynthesis. *Journal of Experimental Marine Biology and Ecology* **203**:3445–3457.

Hoegh-Guldberg O, Mumby PJ, Hooten AJ, Steneck RS, Greenfield P, Gomez E, Harvell CD, Sale PF, Edwards AJ, Caldeira K, Knowlton N, Eakin CM, Iglesias-Prieto R, Muthiga N, Bradbury RH, Dubi A, Hatziolos ME. 2007. Coral reefs under rapid climate change and ocean acidification. *Science* **318**:1737–1742 DOI 10.1126/science.1152509.

Hönisch B, Ridgwell A, Schmidt DN, Thomas E, Gibbs SJ, Sluijs A, Zeebe R, Kump L, Martindale RC, Greene SE, Kiessling W, Ries J, Zachos JC, Royer DL, Barker S, Marchitto Jr TM, Moyer R, Pelejero C, Ziveri P, Foster GL, Williams B. 2012. The geological record of ocean acidification. *Science* **335**:1058–1063 DOI 10.1126/science.1208277.

Jokiel PL. 1978. Effects of water motion on reef corals. *Journal of Experimental Marine Biology and Ecology* **35**:87–97 DOI 10.1016/0022-0981(78)90092-8.

Jokiel PL. 2011a. Ocean acidification and control of reef coral calcification by boundary layer limitation of proton flux. *Bulletin of Marine Science* **87(3)**:639–657 DOI 10.5343/bms.2010.1107.

Jokiel PL. 2011b. The reef coral two compartment proton flux model: a new approach relating tissue-level physiological processes to gross corallum morphology. *Journal of Experimental Marine Biology and Ecology* **409**:1–12 DOI 10.1016/j.jembe.2011.10.008.

Jokiel PL. 2013. Coral reef calcification: carbonate, bicarbonate and proton flux under conditions of increasing ocean acidification. *Proceedings of the Royal Society of London B* **280**:20130031 DOI 10.1098/rspb.2013.0031.

Jokiel PL, Bahr KD, Rodgers KS. 2014. Low-cost, high-flow mesocosm system for simulating ocean acidification with CO_2 gas. *Limnology and Oceanography Methods* In Press.

Jokiel PL, Maragos JE, Franzisket L. 1978. Coral growth: buoyant weight technique. In: Stoddart DR, Johannes RE, eds. *Coral reefs: research methods. (Monographs on oceanographic methodology series, 5)*. Paris: UNESCO, 529–542.

Jokiel PL, Rodgers KS, Kuffner IB, Andersson AJ, Cox EF, Mackenzie FT. 2008. Ocean acidification and calcifying reef organisms: a mesocosm investigation. *Coral Reefs* **27**:473–483 DOI 10.1007/s00338-008-0380-9.

Kaandorp JA, Filatov M, Chindapol N. 2011. Simulating and quantifying the environmental influence on coral colony growth form. In: Dubinsky Z, Stambler N, eds. *Coral reefs: an ecosystem in transition*. New York: Springer Press, 177–185.

Kaandorp JA, Sloot PMA, Merks RMH, Bak RPM, Vermeij MJA, Maier C. 2005. Morphogenesis of the branching reef coral *Madracis mirabilis*. *Proceedings of the Royal Society of London B* **272**:127–133 DOI 10.1098/rspb.2004.2934.

Kinsey D. 1978. Alkalinity changes and coral reef calcification. *Limnology & Oceanography* **23(5)**:989–991 DOI 10.4319/lo.1978.23.5.0989.

Kleypas JA, Buddemeier RW, Archer D, Gattuso JP, Langdon C, Opdyke BN. 1999. Geochemical consequences of increased atmospheric carbon dioxide on coral reefs. *Science* **284**:118–120 DOI 10.1126/science.284.5411.118.

PeerJ

Kühl M, Cohen Y, Dalsgaard T, Jørgensen BB, Revsbech NP. 1995. Microenvironment and photosynthesis of zooxanthellae in scleractinian corals studied with microsensors for O_2, pH and light. *Marine Ecology Progress Series* **117**:159–172 DOI 10.3354/meps117159.

Lesser MP, Weis VM, Patterson MR, Jokiel PL. 1994. Effects of morphology and water motion on carbon delivery and productivity in the reef coral, *Pocillopora damicornis* (Linnaeus): diffusion barriers, inorganic carbon limitation, and biochemical plasticity. *Journal of Experimental Marine Biology and Ecology* **178**:153–179 DOI 10.1016/0022-0981(94)90034-5.

Mass T, Genin A, Shavit U, Grinstein M, Tchernov D. 2010. Flow enhances photosynthesis in marine benthic autotrophs by increasing the efflux of oxygen from the organism to the water. *Proceedings of the National Academy of Sciences of the United States of America* **107**:2527–2531 DOI 10.1073/pnas.0912348107.

McMahon A, Santos IR, Cyronak T, Eyre BD. 2013. Hysteresis between coral reef calcification and the seawater aragonite saturation state. *Geophysics Research Letters* **40**:4675–4679 DOI 10.1002/grl.50802.

Mehrbach C, Culberson CH, Hawley JE, Pytkowicz RM. 1973. Measurement of the apparent dissociation constants of carbonic acid in seawater at atmospheric pressure. *Limnology & Oceanography* **18**:897–907 DOI 10.4319/lo.1973.18.6.0897.

Murillo LJA, Jokiel PL, Atkinson MJ. 2014. Alkalinity to calcium flux ratios for corals and coral reef communities: variances between isolated and community conditions. *PeerJ* **2**:e249 DOI 10.7717/peerj.249.

Odum HT, Odum EP. 1955. Trophic structure and productivity of a windward coral reef community on Eniwetok Atoll. *Ecological Monographs* **25**:291–320 DOI 10.2307/1943285.

Pierrot D, Lewis E, Wallace DWR. 2006. MS Excel Program Developed for CO_2 System Calculations. Carbon Dioxide Information Analysis Center, Oak Ridge National Laboratory, U.S. Department of Energy, Oak Ridge, Tennessee DOI 10.3334/CDIAC/otg.CO2SYS_XLS_CDIAC105a.

Price NN, Martz TR, Brainard RE, Smith JE. 2012. Diel Variability in seawater pH relates to calcification and benthic community structure on coral reefs. *PLoS ONE* **7**(**8**):e43843 DOI 10.1371/journal.pone.0043843.

Roleda MY, Boyd PW, Hurd CL. 2012. Before ocean acidification: calcifier chemistry lessons. *Journal of Phycology* **48**:840–843 DOI 10.1111/j.1529-8817.2012.01195.x.

Schneider K, Erez J. 2006. The effect of carbonate chemistry on calcification and photosynthesis in the hermatypic coral *Acropora eurystoma*. *Limnology & Oceanography* **51**:1284–1293 DOI 10.4319/lo.2006.51.3.1284.

Shamberger KEF, Cohen AL, Golbuu Y, McCorkle DC, Lentz SJ, Barkley HC. 2014. Diverse coral communities in naturally acidified waters of a Western Pacific Reef. *Geophysical Research Letters* **41**(**2**):499–504 DOI 10.1002/2013GL058489.

Shamberger KEF, Feely RA, Sabine CL, Atkinson MJ, DeCarlo EH, Mackenzie FT, Drupp PS, Butterfield DA. 2011. Calcification and organic production on a Hawaiian coral reef. *Marine Chemistry* **127**:64–75 DOI 10.1016/j.marchem.2011.08.003.

Shashar N, Cohen Y, Loya Y. 1993. Extreme diel fluctuations of oxygen in diffusive boundary layers surrounding stony corals. *Biological Bulletin* **185**:455–461 DOI 10.2307/1542485.

Shashar N, Kinane S, Jokiel PL, Patterson MR. 1996. Hydromechanical boundary layers over a coral reef. *Journal of Experimental Marine Biology and Ecology* **199**:17–28 DOI 10.1016/0022-0981(95)00156-5.

Silverman J, Lazar B, Cao L, Caldeira K, Erez J. 2009. Coral reefs may start dissolving when atmospheric CO_2 doubles. *Geophysical Research Letters* **36**:L05606 DOI 10.1029/2008GL036282.

Smith SV, Kinsey DW. 1978. Calcification and organic carbon metabolism as indicated by carbon dioxide. In: Stoddart DR, Johannes RE, eds. *Coral reefs: research methods. (Monographs on oceanographic methodology series, 5)*. Paris: UNESCO, 469–484.

Smith SV, Jokiel PL, Key GS, Guinther EB. 1977. *Metabolic responses of shallow tropical benthic microcosm communities to perturbation.* Environmental Protection Agency, Narragansett, Rhode Island. Final report of contract R800906. 110 pp. *Available at http://cramp.wcc.hawaii.edu/.*

Suzuki A, Nakamori T, Kayanne H. 1995. The mechanism of production enhancement in coral reef carbonate systems: model and empirical results. *Sedimentary Geology* **99**:259–280 DOI 10.1016/0037-0738(95)00048-D.

Weis VM, Smith GJ, Muscatine LA. 1989. "CO_2 supply" mechanism in zooxanthellate cnidarians: role of carbonic anhydrase. *Marine Biology* **100**:195–202 DOI 10.1007/BF00391958.

Wooldridge S. 2013. A new conceptual model of coral biomineralisation: hypoxia as the physiological driver of skeletal extension. *Biogeosciences* **10**:2867–2884 DOI 10.5194/bg-10-2867-2013.